Light Scattering By Random, Irregular Shaped Terrigenous Sediment Particles

Yogesh C. Agrawal and H.C. Pottsmith
Sequoia Scientific, Inc., 2700 Richards Road, Bellevue, Wa 98005 USA. email: yogi.agrawal@sequoiasci.com

Amanda Briggs Whitmire
Oregon State University, Corvallis, OR USA. email: abriggs@coas.oregonstate.edu

ABSTRACT

This work is motivated by the need to understand particle shape effects for measurement of size distribution of suspended sediments. Although the light scattering properties of natural, random shaped and randomly oriented ensemble of particles are fundamentally important, the present perspective is from the method of laser diffraction. Laser diffraction is a widely used principle for sizing particles in research and industry. The LISST-100 instruments manufactured by Sequoia Scientific, Inc. of Bellevue, Washington employ this principle for in-situ measurements of suspended particles. The broad applicability of the method is rooted in the idea that small-angle scattering by spheres, described by Mie theory, is identical to diffraction through an equal-diameter aperture. Consequently, particle composition, which is represented by refractive index, is mostly immaterial. Departure from sphericity, on the other hand, is known to damp the oscillations of Mie theory, but is not fully predictable from theory for arbitrarily large sediment grains. We report here systematic qualitative and quantitative differences between light scattering properties of homogeneous spheres, vs. random shaped natural particles. The findings are that natural particles appear about ¼ to ½ ϕ larger than spheres passing identical sieves, and light scattering by a single-size natural particle is equivalent to a broad distribution of spheres. A limited study of natural particles from different sources suggests minor differences, again. These and other differences from spheres are described.

INTRODUCTION

Light scattering by particles is fundamental to many disciplines of physics, including atmospheric and oceanic inherent optical properties. Mie theory describes scattering by homogeneous spheres without limitations on size or refractive index. Extensions to layered, hollow etc. types of particles exist in literature. The present interest is in the properties of randomly oriented, randomly shaped sediment particles, from the standpoints of particle sizing and backscattering for remote sensing. These properties constitute the inherent optical properties associated with particles, which underlie the volume scattering function of water. In the present work, we are exploring the small-angle scattering part of the inherent optical properties.

The literature on non-spherical but *regular* shaped particles is growing. This is represented by work presented by and recently , both driven by the particle sizing problem. Many other contributions on this topic are in texts,such as . Earlier, a group lead by Jones worked out an elegant set of solutions for random shaped apertures, , , which applies to highly absorbing particles only. At the time, the laser diffraction method itself employed the diffraction formulation to model light scattering by spheres (obviously, before plentiful computing power made Mie theory models practical). Jones' solutions did not find practical use since they were purely diffraction based. Theoretical access to random large particles (*ka>100*) does not exist today, hence we have chosen the empirical route.

Presented at Ocean Optics XVIII, Montreal, Canada, Oct9-13, 2006.

In the present work, we represent small-angle scattering in transformed variables, which illustrate differences from spheres more clearly. Instead of using the logarithmic ordinate for Mie theory, which hides differences, a weighted integral I is employed such that the transformed quantity is:

$$I = \int \{i_1 + i_2\}\ \theta\ \mathrm{d}\theta \qquad (1)$$

Here, the properties in curly brackets are well known in the optics community from Mie theory (Van de Hulst, 1982). Integration limits are small, selected in logarithmic intervals, which ensures: (*i*) that the main and subsequent 3 Mie scattering lobes are visible, and (*ii*) in log-angle space, the rows of a kernel matrix (see later) whose elements are described by eq. (1) become similar . In figure 1 below, we show the transformation of the Mie scattering curves to this new variable via eq. 1, which can now be displayed in a linear ordinate.

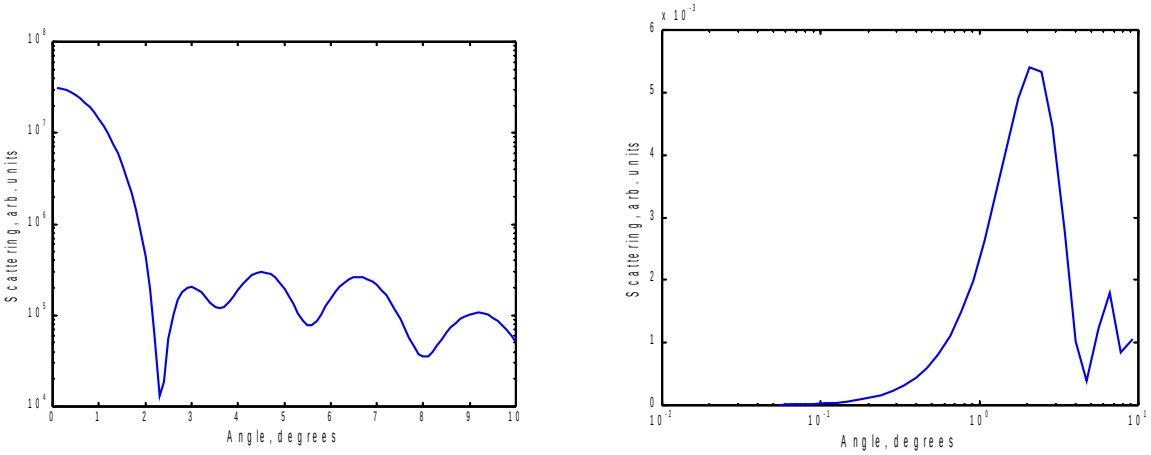

Figure 1: Light scattering by a 10 micron particle, Mie theory (left), and a transformed plot showing linear ordinate and logarithmic abscissa(right). Note that the first lobe of Mie plot transforms to the main maximum on right, and subsequent maxima are visible as weaker peaks.

The particle sizing problem uses this linear-ordinate formulation. The left hand variable I in eq. (1) is then one element in a kernel matrix. In general, for the sake of completeness, we note that an element $K_{i,j}$ in the laser diffraction kernel matrix is defined by:

$$K_{i,j} = \int a^{-\alpha}\, \mathrm{d}a \int \{i_1 + i_2\}\ \theta\ \mathrm{d}\theta \qquad (2)$$

where integration in θ and a is over sub-ranges of angles θ and sizes a. For explanation of α, see below. Further details are presented by Agrawal and Pottsmith (2000).

This kernel matrix relates the light scattering properties of particles with their size distribution as follows;

$$\underline{E} = \mathbf{K}\,\mathbf{C} \qquad ; \qquad (3)$$

where $\underline{E}$ is the scattered energy sensed by the multi-angle scattering sensors of a laser diffraction instrument such as the LISST-100, **K** is the kernel matrix, and **C** is the size distribution vector, each

element of which is the concentration of a particular size class. When **C** is in area concentration (cm^2/l), α=3, and the matrix **K** is near symmetric. When **C** is in volume or mass concentration (cm^3/l, g/l), α=4.

LISST instruments measure multi-angle scattering E of Eq. 3, and beam attenuation through a 5 cm path length of water (shorter or longer paths are sometimes employed, respectively, for high or low particle concentrations). The beam attenuation is used for de-attenuating the measured multi-angle scattering, although by itself this is a high-accuracy measure of beam attenuation coefficient due to the small acceptance aperture for attenuation measurements (see Boss & Slade, this volume).

Returning to light scattering properties, it is noted that each row of the kernel matrix **K** represents scattering into the different ring detectors by a narrow range of particle sizes. Thus, a comparison of Mie theory and natural particle scattering amounts to a comparison of data collected with spheres (amply verified against Mie theory, see ,) and by natural particles. This is what has been done for the present work.

The data presented in this abstract show small-angle scattering by spheres and natural particles per unit volume concentration in narrow size ranges (¼ ϕ wide; one ϕ is a factor of 2 on log scale; ¼ ϕ means a factor of 1.19). An examination of the variability of scattering by natural particles originating in different sources is only shown for coarse sorting at this time. Variability depending on particle source at high resolution in sizes will follow in a subsequent report.

METHODS

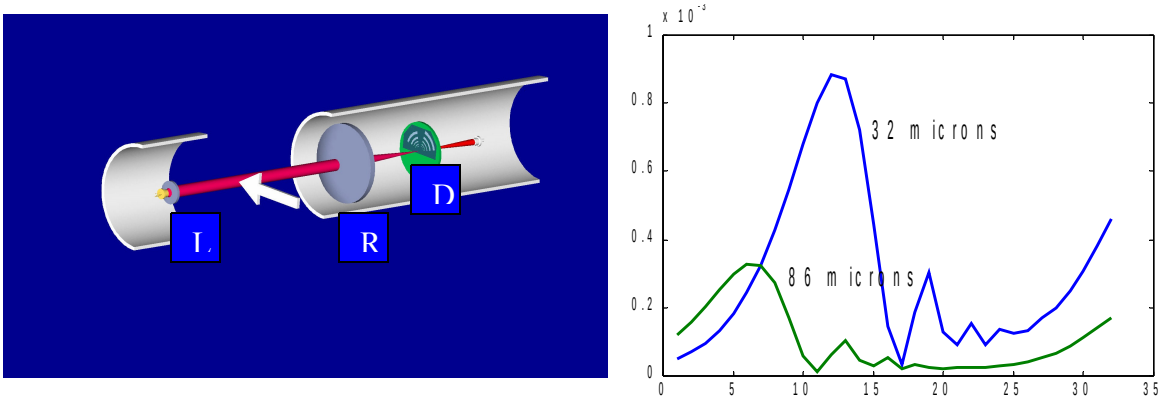

Figure 2: left: Optics of a LISST-100 showing laser (L), receive lens (R) and detector (D); right: scattering per unit volume concentration of two distinct size spheres. Note the similarity of shape, and 1/a dependence of magnitudes.

We have employed a LISST-100 instrument. A schematic of the optics, the collimated laser beam, the receive lens, the multi-ring detector, and the beam attenuation sensor is displayed in Fig. 2. Particles were sorted by sieving or in a settling column. Although particles from a few other sources have been examined, here we restrict the results to data using sediments from the Satluj River, India, available to us in relation to grain size monitoring at a dam site on this river. The particles were sorted in to ¼-ϕ size classes (or size bins) from 500 microns to 16 microns using sieves. Sieving below 16 microns was found to be impractical. For this reason, particles below 16 microns are being studied by sorting in a

settling column. Thus, note that the sub-16 sizes are 'settling' sizes, against 'sieved' sizes above 16 microns. Sieved particles in any size-bin were suspended in known mass concentration in the small mixing chamber of a LISST-100 and the multi-angle scattering was measured. Simultaneously, glass spheres were sieved through identical sieves to obtain parallel size distributions above 16 microns. This latter procedure also provided a method to calibrate the system for finer spheres.

RESULTS AND CONCLUSION

The first key result concerns the shape, location, and magnitude of scattering by random particles contrasted with spheres. This is shown in Figure 3. Comparing with scattering signatures of Fig.2 reveals 4 differences: (*i*) the secondary maxima associated with spheres vanish for random particles, (*ii*) the peak of scattering shifts to the left for random shapes, , (*iii*) the magnitude of the peak for random shapes is reduced, and , (*iv*) the shape shows a widening of the principal peak.

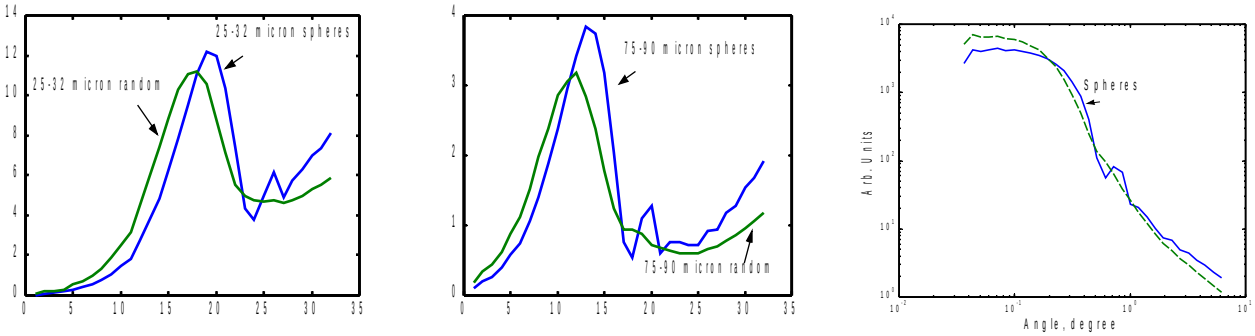

***Figure 3: Comparison of scattering per unit concentration for spheres and random particles, size bin 25-32 microns (left) and 75-90 microns (center). Abscissa is detector ring number. On right, the data of center is shown in conventional Mie plot, which de-emphasizes the difference.* (*Data collected with 750 micron upper limit instrument.*)**

We have explained in the past that the location of the peak crudely reflects the mean size of particles. This suggests that random shaped particles, *sieved through identical sieves as spheres,* appear larger. The shift is 1 to 2 detectors, which correspond to ¼ to ½ ϕ in sizes. In other words, the first significant result is that random shaped particles appear larger by ¼ to ½ ϕ than spheres sieved into the same size bin. Such observations were reported by in a 'black-box' study of similarly sorted sediments. The present study is looking inside this 'black box'. The missing secondary maximum in scattering from natural shapes is understandable as a reduction in order associated with loss of order in shape. Notably though, the larger particles (Fig. 3, *center*) show a hint of a secondary peak – a feature that is sustained all the way to sizes up to 500 microns.

The magnitude of the peak of scattering from random particles is seen to be smaller, however the ratio of the total energy in scattering (area under the curves, spheres/random) is in the ratio 99.9% for the finer particles and 113% for the larger fraction. These are to be treated to be within the errors of measurement introduced by variability of mixing. The challenge of thorough mixing is well known to scientists working with particles.

The widening of the shape of scattering for random shapes can be intuitively understood with a reference to the Airy pattern of circular apertures. A random shape includes smaller and larger apertures. With sieved samples, the maximum dimension can be larger as some particles pass through sieves with their longer axis aligned normal to the hole aperture. The smaller dimension can clearly be smaller than the aperture opening. Thus, the smaller dimension can produce the wider diffraction, while the longer axis can produce the narrower pattern. The net result is broadening.

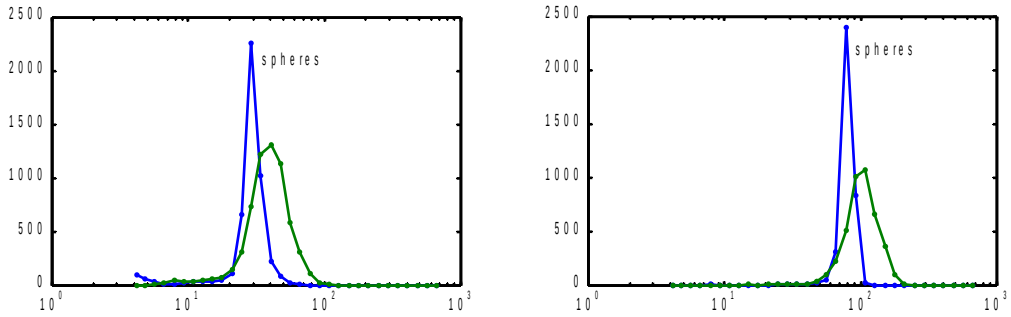

Figure 4: Equivalent spheres size distribution for data of Fig.2. Note the shift and broadening due to shape effects. Left: 25-30 microns fraction; right: 75-90 microns.

The size distributions of the data displayed in Figure 3 is displayed in Figure 4. The inversions are performed with a matrix computed for spheres, producing equivalent sphere results. Clearly, natural particles that passed the same sieves as spheres appear larger, and of broad distribution when viewed as equivalent spheres.

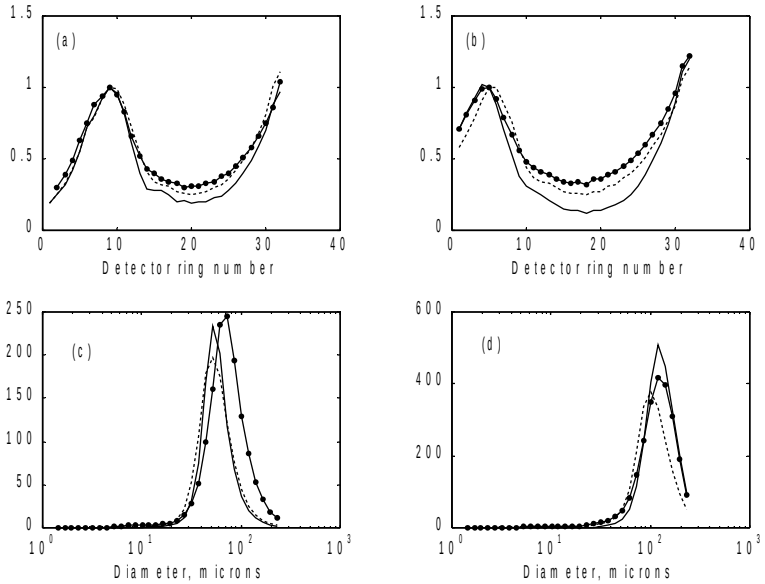

Figure 5: Variability of multi-angle scattering for various particles.(a) 32-63 micron particle scattering across detector rings; (b) same, but for 63-125 micron particles; (c) and (d), size distribution for (a) and (b) respectively. For all figures, solid line: USGS particles, -- PTI, .- Satluj.

We next display scattering by particles obtained from different sources, but sorted through identical sieves. The data now are for coarse fractions, 1-ϕ wide. Again, scattering per unit volume concentration of particles is displayed, Fig.5. In this case, to emphasize differences in shape for

viewing, the scattering is normalized at the peak. The most noticeable difference is in the depth of the minimum scattering. The deepest minima are seen to occur for particles labeled 'USGS'. These aeolian particles have rounder edges, (see Fig. 6). Particles from the two other sources – PTI and Satluj river, India, show nearly identical scattering signatures. The equivalent sphere sizes show minor discrepancy as well, the USGS particles exhibiting slightly narrower size distribution. With further data, it may emerge that due to this variability, a 'natural particle' matrix may be formed to replace equivalent sphere inversion with random particles, but with not the full resolution in sizes due to the variability of the scattering signatures.

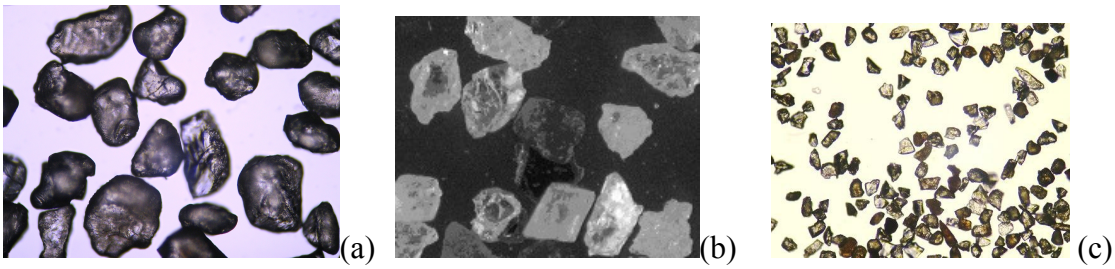

Fig. 6: Photos of particles sieved into 125-250 micron size bin, (a) rounded particles from an unknown source in South Dakota (provided by USGS), and (b) rough particles from Satluj river, India; (c) Arizona dust particles from PTI (32-64 micron).

Further details will be presented at the meeting, including a discussion of the apparent backscatter optical cross-sections derived from equivalent sphere populations for natural sediments, with clear implications to remote sensing.

REFERENCES

Van de Hulst, 1982: Light scattering by small particles, Dover, pp. 470.